Turkish Journal of Physics

http://journals.tubitak.gov.tr/physics/

Research Article

Turk J Phys
(2018) 42: 378 – 385

doi:10.3906/fiz-1802-27

The investigation of the lattice strains and crystallite sizes of Y358 and Y123 high-temperature superconductors

İbrahim DÜZGÜN*
Department of Physics Engineering, Faculty of Engineering, Gümüşhane University, Gümüşhane, Turkey

Received: 16.02.2018 • **Accepted/Published Online:** 18.06.2018 • **Final Version:** 15.08.2018

Abstract: In this study, the Y358 phase, the newest high-temperature superconductor member of the yttrium barium copper oxide family, was produced using the solid-state reaction technique. The Y358 superconductor exhibited the Meissner effect at low temperature (77 K). The X-ray diffraction spectra indicated that the crystal structure was almost identical to that of Y123, but with some impurity peaks. An X-ray peak broadening analysis was applied to determine the lattice strain, and the medial crystallite size was calculated perpendicular to the surface of the superconductor specimens. As a result of the analyses, it was determined that the crystallite size of the Y358 superconductor was about 1.125 times larger than that of the Y123 superconductor.

Key words: High-Tc superconductor, Y123, Y358, crystallite structure, lattice parameters

1. Introduction

In 1987, Chu et al. discovered $YBa_2Cu_3O_7$ (Y123). This superconductor, with a transition temperature (T_c) of nearly 90 K, comprises double CuO_2 planes and a single CuO chain [1,2]. Since its discovery, Y123 has been the most frequently researched compound of the yttrium barium copper oxide (YBCO) family. In 1988, two more compounds joined this family: $YBa_2Cu_4O_8$ (Y124), with a T_c of 80 K, and $Y_2Ba_4Cu_7O_{15}$ (Y247), with a T_c of 40 K [3,4]. The superconductor Y124 possesses a bilayer CuO_2 plane and two CuO chains, while Y247 includes a bilayer CuO_2 plane, a single CuO chain, and a double CuO chain between the CuO_2 planes [5]. With every high-temperature superconductor (HTSC), when the number of the CuO_2 planes increases, the T_c rises [6]. The most recently added superconducting member of the YBCO family, Y358, exhibits a T_c of $\geq$100 K [7]. This phase has five CuO_2 planes and three CuO chains, divided into two sets, with three CuO_2 planes separated by BaO layers from the other two CuO_2 planes, thus differing from similar cuprates in this regard [8]. Some studies investigated the crystal structure and electrical [9], superconducting, and transport [10] properties of the Y358 compound.

The present study is the first to compare Y123 and Y358 HTSCs in terms of lattice strain and crystallite size. By employing a diffractometer, the X-ray diffraction peak broadening is clearly seen in the obtained patterns. Upon analysis, this broadening becomes quantifiable. Thus, it is significant to note that instrumental effects, along with lattice strain and crystallite size, are the primary reason for the diffraction peak broadening. Scherrer derived a formula for this X-ray diffraction peak broadening applicable for small-sized crystallites [11],

*Correspondence: ibrahimduzgun@gumushane.edu.tr

as shown in Eq. (1):

$$B_{crystallite} = \mu\lambda/L\cos\theta, \tag{1}$$

where λ is the X-ray wavelength, L is the medial crystallite size measured perpendicular to the surface of the specimen, θ is the Bragg angle, and μ is a constant (usually taken to be 0.89 for spherical particles).

It should be noted that diffraction peak broadening is also caused by the lattice strain of the compound. This can be expressed by Eq. (2):

$$B_{strain} = \eta\tan\theta, \tag{2}$$

where η is the strain in the compound [12].

In the current study, an X-ray peak broadening analysis of the superconductor specimens was conducted to determine the lattice strain, and the average crystallite size was calculated perpendicular to the surface.

2. Materials and methods

The experimental procedure of the current study is the same as that of the previously described study [7], of which the following is a summary: Employing the well-known solid-state reaction (SSR) technique, $Y_3Ba_5Cu_8O_{18+}$ (Y358) and $YBa_2Cu_3O_{7-x}$ (Y123) compounds were synthesized under the same conditions. The calculated amounts of CuO, Y_2O_3, and $BaCO_3$ powders were mixed and ground together. The reaction was completed within 12 h at 840 °C. The samples were cooled for 5 h to room temperature. Calcination was performed twice during the middle grinding session and the pellets were formed after the powder was ground once more. Pellets (12 mm diameter × 1 mm thickness) were prepared under 10 t/cm^2 pressure. The sintering temperature was determined via TGA and DTA analysis. The synthesis of the samples was then completed in an oxygen atmosphere at 800–1000 °C for 24 h and the system was cooled to 500 °C. After the samples were held in oxygen for approximately 10 h, they were further cooled down until room temperature was reached. A JEOL JSM 6610 scanning electron microscope (SEM) was used for morphological information. Compositional analysis was studied by an Oxford Instruments Inca X-act energy dispersive X-ray spectroscope attached to the SEM. The samples were subjected to X-ray diffraction (XRD) via a Rigaku D/Max-IIIC diffractometer to determine the structure of the crystals. The CuK_α radiation (λ = 1.54059 Å) of the diffractometer ranged from 20° to 60° at a rate of 0.2° min^{-1} at room temperature. After cooling the samples down to 77 K (the temperature of liquid nitrogen), their superconducting behavior was confirmed by observing the Meissner effect.

3. Results and discussion

The wide-scale physical properties including texture, stress, crystallinity, and crystallite sizes of the synthesized samples were established via the X-ray patterns. The essential application of XRD to the HTSCs was to determine the underlying phases. The Y358 and Y123 XRD patterns are displayed in Figure 1. The crystal structure of the Y358 phase was orthorhombic, with the Pmm2 space group. The symmetries were in agreement with the literature findings [5,7]. Additionally, the parameters of the lattice were calculated for the Y358 phase via the readjustment process, using Eq. (3):

$$(a, b, c) = (3.892, 3.822, 31.244)\ \text{Å}. \tag{3}$$

The unit cell volume was found using Eq. (4):

$$V = 464.76\ \text{Å}^3. \tag{4}$$

The values of 'a' and 'b' were consistent with those of the studies in the literature [5,7], and 'c' was also in agreement with the previously reported values [8,9,13,14].

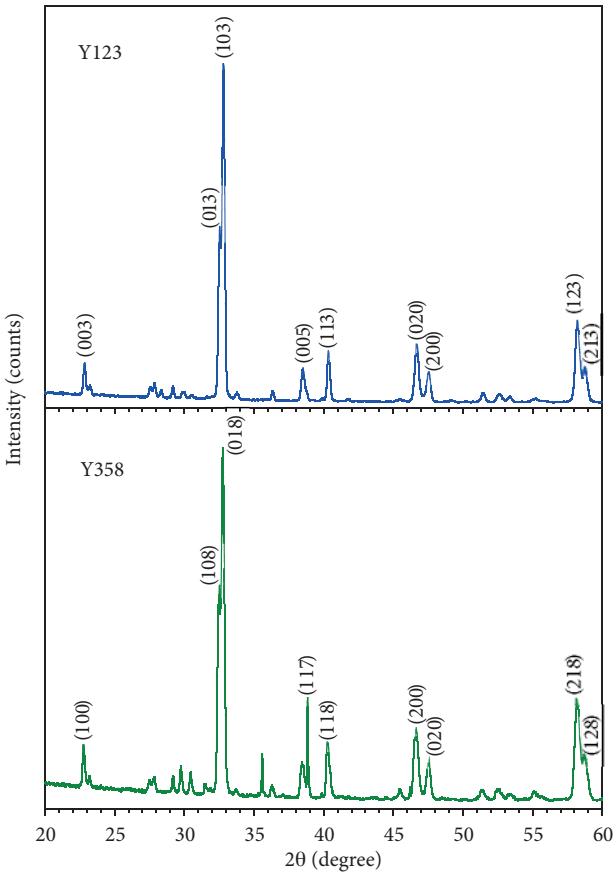

Figure 1. XRD patterns of Y123 and Y358 compounds.

The intercept ($\mu\lambda$ / L) and slope (η) in Figures 2 and 3 were used to calculate the lattice strain (η) and crystallite size (L) from the XRD patterns of the Y123 and Y358 compounds (Figure 1). As a result, the crystallite size of the Y358 superconductor was about 1.125 times larger than that of the Y123 superconductor. The main aim of the current study was to attempt to resolve such discrepancies. After performing the analyses, samples in which the two phases coexisted were prepared. The presence of both phases was confirmed by XRD assisted by standard theoretical treatments. This research, which included other experiments on resistivity vs. temperature, was able to separate the two superconducting phases of Y123 and Y358 and determine their associated properties such as the lattice parameters. The results of this study quite closely parallel those of a previous study [10], where Ayaş et al. clearly defined the characteristics of the Y358 superconductor. The value η for Y358 was greater than that of Y123 at a rate of 34/10,000. When Figure 1 is examined, it can be seen that the diffraction peaks have nearly the same width due to the fact that the contribution from the lattice strain is negligible. Using the intercept ($\mu\lambda$ / L) and slope (η) in Figures 2 and 3, the lattice strain (η) and crystallite size (L) can be calculated from the XRD patterns of the Y123 and Y358 compounds (Figure 1), which are shown in Tables 1 and 2.

For a more detailed analysis, SEM images of the samples and DTA graphs were created and presented. Figures 4a and 4b show the upper surface SEM images, which were magnified by 400 times, of Y123 and Y358

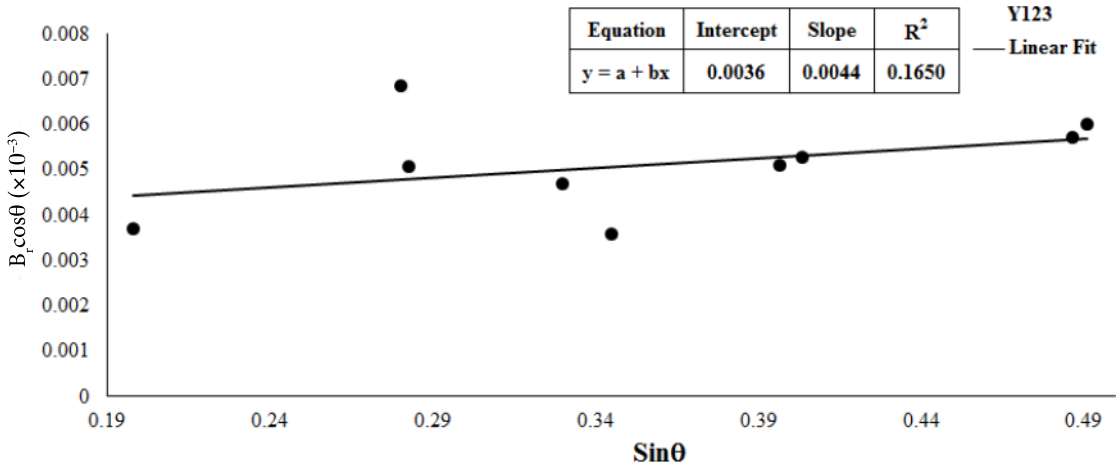

Figure 2. Plot of $B_r \cos\theta$ versus $\sin\theta$ for Y123.

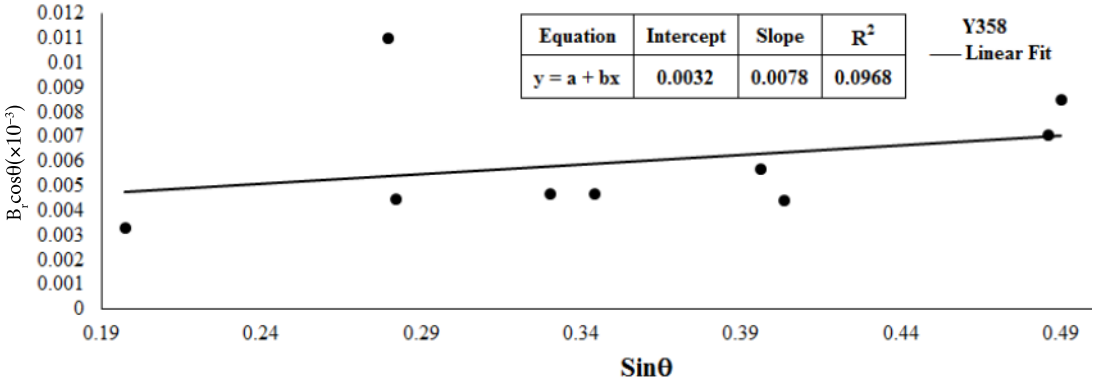

Figure 3. Plot of $B_r \cos\theta$ versus $\sin\theta$ for Y358.

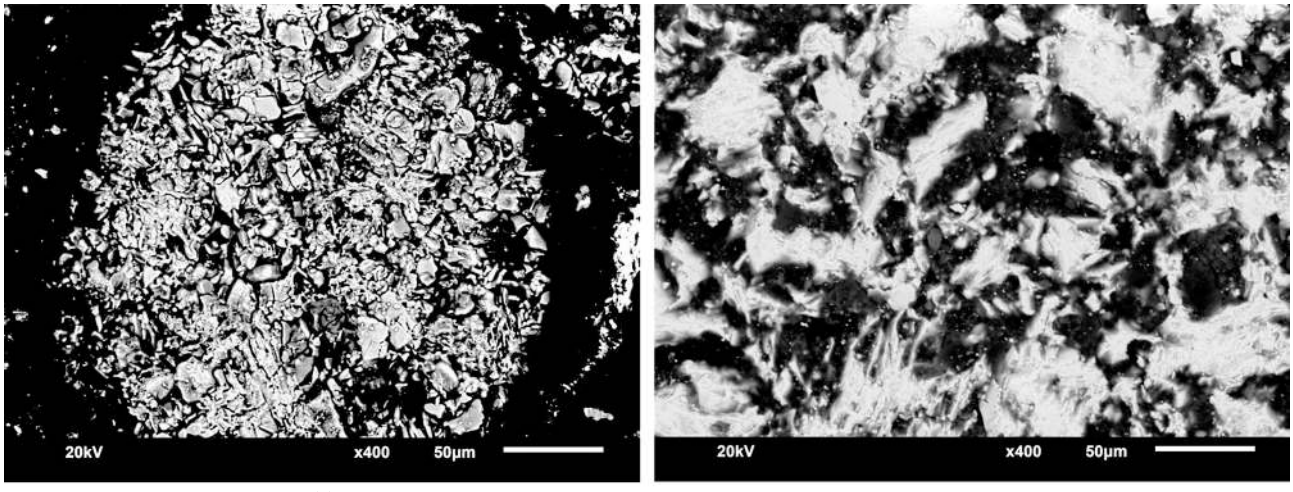

(a) **(b)**

Figure 4. SEM images: Y123 sample (a), Y358 sample (b).

Table 1. The lattice parameters of the samples Y123 and Y358.

Sample	a (Å)	b (Å)	c (Å)	d	h	k	l
Y123	3.819495	3.886493	11.679030	3.8896	0	0	3
				2.7494	0	1	3
				2.7267	1	0	3
				2.3356	0	0	5
				2.2322	1	1	8
				1.9423	0	2	0
				1.9096	2	0	0
				1.5830	1	2	3
				1.5686	2	1	3
Y358	3.892704	3.821956	31.310980	3.9096	1	0	0
				2.7543	1	0	8
				2.7315	0	1	8
				2.3341	1	1	7
				2.2382	1	1	8
				1.9459	2	0	0
				1.9097	0	2	0
				1.5853	2	1	8
				1.5716	1	2	8

Table 2. The lattice strains and crystallite sizes of the samples Y123 and Y358.

$\sin\theta$ (Y123)	$B_r\cos\theta$ (Y123)	$\sin\theta$ (Y358)	$B_r\cos\theta$ (Y358)
0.19804228	0.00369524	0.19717827	0.003336575
0.28016747	0.00685251	0.27966983	0.011026001
0.28249633	0.00507294	0.28200658	0.004504380
0.32980599	0.00469588	0.33001194	0.004695518
0.34508034	0.00358748	0.34415955	0.004703095
0.39658719	0.00509502	0.39586608	0.005689763
0.40337761	0.00528619	0.40336963	0.004439774
0.48660224	0.00571785	0.48588544	0.007108630
0.49106644	0.00602076	0.49014329	0.008519292
η (Y123)	η (Y358)	L [nm] (Y123)	L [nm] (Y358)
0.0044	0.0078	38.0868	42.8477

samples, respectively. The gray color represents grain and the black color shows porosities in the images. It was observed that the grain size of Y358 was larger than those of Y123. It is known that compounds that have relatively larger grain size have better superconducting properties such as critical current density and levitation force density [15].

Figures 5a and 5b show the upper surface EDX spectra of Y123 and Y358 samples, respectively. It was confirmed that the samples contained Y, Ba, Cu, and O elements according to the data obtained from

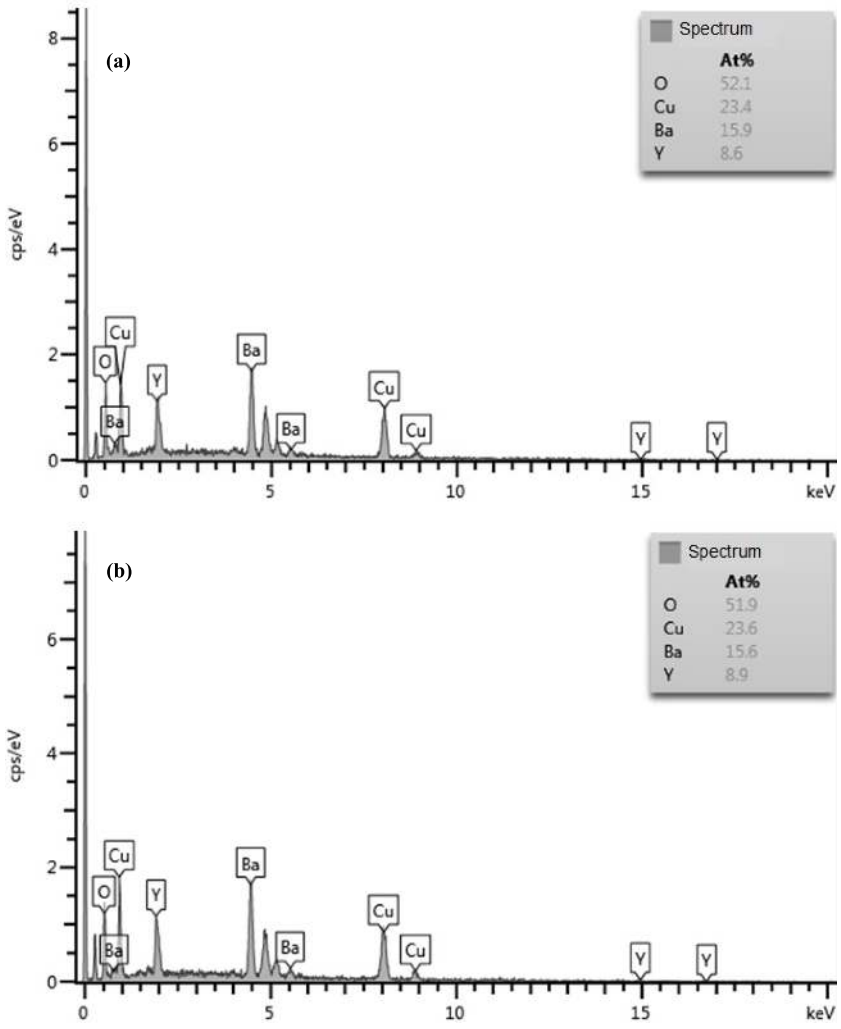

Figure 5. EDX spectra: Y123 sample (a), Y358 sample (b).

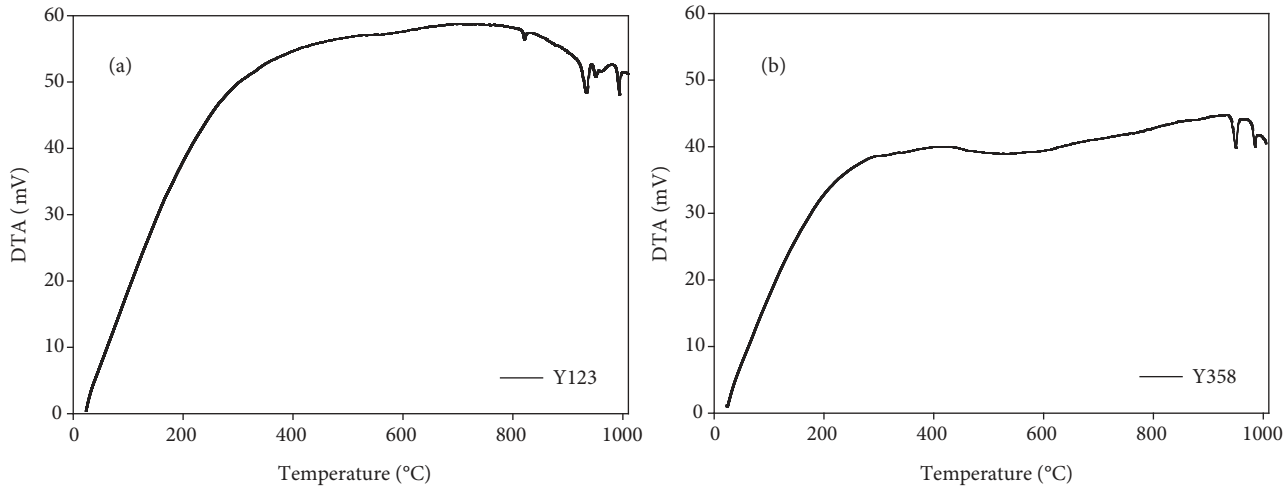

Figure 6. DTA graphs: Y123 sample (a), Y358 sample (b).

the gray color. Besides, the chemical formulations of Y123 and Y358 determined by atomic percentages were $YBa_{1.85}Cu_{2.72}O_x$ and $Y_{3.00}Ba_{5.25}Cu_{7.95}O_y$, respectively. Here, oxygen was not taken into account as its atomic number is less than 11 [16]. The obtained data are in a good agreement with those in the literature [2,17]. For evaluating the sintering processes, the DTA measurements of the Y123 and Y358 were determined as in Figure 6. The peaks at 800–1000 °C are related to the formation of the liquid phase and the decomposition temperature of Y123 and Y358 compounds. Through these results, the melting temperature and crystal-growth temperature in the sintering process were respectively chosen to be 930 °C and 950 °C.

4. Conclusion

This study is the first to compare the lattice strains and crystallite sizes of Y123 and Y358 HTSCs. The findings obtained in the current study are quite consistent with the data published in the literature. It was determined that the crystallite size of the Y358 superconductor was about 1.125 times greater than that of the Y123 superconductor, whereas the lattice strain of Y358 was only slightly larger than that of Y123. This very small difference confirms the notion that the contribution of the lattice strain can safely be disregarded. Consequently, it can be concluded that using X-ray diffraction to detect the difference in the lattice strains is problematical.

Acknowledgment

The author wishes to thank Gümüşhane University for supporting the present study with a Gümüşhane University Research Fund (GÜBAP) grant (Project Number: 13.F5120.02.1).

References

[1] Chu, C. W.; Hor, P. H.; Meng, R. L.; Gao, L.; Huang, Z. J.; Wang, Y. Q. *Phys. Rev. Lett.* **1987**, *58*, 405-407.

[2] Kutuk, S.; Bolat, S.; Terzioglu, C.; Altintas, S. P. *J. Alloy. Compd.* **2015**, *650*, 159-164.

[3] Marsh, P.; Fleming, R. M.; Mandich, M. L.; DeSantolo, A. M.; Kwo, J.; Hong, M.; Martinez-Miranda, L. J. *Nature* **1988**, *334*, 141-143.

[4] Bordet, P.; Chaillout, C.; Chenavas, J.; Hodeau, J. L.; Marezio, M.; Karpinski, J.; Kaldis, E. *Nature* **1988**, *334*, 596-598.

[5] Aliabadi, A.; Akhavan-Farshchi, Y.; Akhavan, M. *J. Supercond. Nov. Magn.* **2014**, *27*, 741-748.

[6] Nakajima, S.; Kikuchi, M.; Syono, Y.; Oku, T.; Shindo, D.; Hiraga, K.; Kobayashi, N.; Iwasaki, H.; Muto, Y. *Physica C* **1989**, *158*, 471-476.

[7] Aliabadi, A.; Akhavan-Farshchi, Y.; Akhavan, M. *Physica C* **2009**, *469*, 2012-2014.

[8] Gholipour, S.; Daadmehr, V.; Rezakhani, A. T.; Khosroabadi, H.; Tehrani, F. S.; Akbarnejad, R. H. *J. Supercond. Nov. Magn.* **2012**, *25*, 2253-2258.

[9] Topal, U.; Akdogan, M.; Ozkan, H. *J. Supercond. Nov. Magn.* **2011**, *24*, 2099-2102.

[10] Ayaş, A. O.; Ekicibil, A.; Çetin, S. K.; Coşkun, A.; Er, A. O.; Ufuktepe, Y.; Fırat, T.; Kıymaç, K. *J. Supercond. Nov. Magn.* **2011**, *24*, 2243-2252.

[11] Scherrer, P. *Nachr. Ges. Wiss. Göttingen* **1918**, *26*, 98-100.

[12] Suryanarayana, C.; Norton, M. G. *X-Ray Diffraction: A Practical Approach*; Plenum Press: New York, NY, USA, 1998.

[13] Udomsamuthirun, P.; Kruaehong, T.; Nikamjon, T.; Ratreng, S. *J. Supercond. Nov. Magn.* **2010**, *23*, 1377-1380.

[14] Başoğlu, M.; Düzgün, İ. *J. Supercond. Nov. Magn.* **2016**, *29*, 1737-1740.

[15] Salama, K.; Lee, D. F. *Supercond. Sci. Tech.* **1994**, *7*, 177.

[16] Kutuk, S.; Kutuk-Sert, T. *Arab. J. Sci. Eng.* **2017**, *42*, 4801-4809.

[17] Bolat, S.; Kutuk, S. *J. Supercond. Nov. Magn.* **2012**, *25*, 731-738.